JSE Journal of Systematics and Evolution

doi: 10.1111/jse.13123

Research Article

# Genomic differentiation and gene flow among *Rattus* species distributed in China and adjacent regions

Ning Liu[1,2], Xin-Lai Wu[1,2], Ruo-Bing Zhang[1,3], Jin Wang[1,2], Qi-Sen Yang[1], Ji-Long Cheng[1], Zhi-Xin Wen[1], Lin Xia[1], Alexei V. Abramov[4]*, and De-Yan Ge[1]*

[1]Key Laboratory of Zoological Systematics and Evolution, Institute of Zoology, Chinese Academy of Sciences, Beijing 100101, China
[2]College of Life Sciences, University of Chinese Academy of Sciences, Beijing 100049, China
[3]Xinjiang Key Laboratory of Biological Resources and Genetic Engineering, College of Life Science and Technology, Xinjiang University, Urumqi 830046, China
[4]Zoological Institute, Russian Academy of Sciences, Saint Petersburg 199034, Russia
*Authors for correspondence. Alexei V. Abramov. E-mail: a.abramov@mail.ru; De-Yan Ge. E-mail: gedy@ioz.ac.cn
Received 18 April 2024; Accepted 15 June 2024

**Abstract** The wild rats in the genus *Rattus* represent a group of murids characterized by rapid lineage diversification but limited morphological variation. Within this genus, there are several commensal species with high invasive capacity, such as *Rattus norvegicus* and *R. rattus*, which pose a global threat. Investigating the mechanisms behind their adaptive evolution is of utmost importance. In this study, we conducted morphological study and whole-genome sequencing on *Rattus* species distributed in China and adjacent regions to gain insights into morphological differentiation, as well as genomic divergence and gene flow using assembled mitochondrion genome and high-quality single nucleotide polymorphisms. Despite their morphological similarity and large overlap in morphospace, our analyses revealed significant genetic differentiation at the genomic level among *Rattus* species in China and adjacent regions. Specifically, intraspecific differentiation was observed in *R. nitidus*, *R. norvegicus*, and *R. tanezumi*, which may be related to habitat heterogeneity and geographic isolation. We hypothesize that as invasive rats expand their habitat, the diversification of ecological environments might lead to more environmentally adapted evolution and accelerated genetic differentiation. Furthermore, Dsuite and TreeMix analyses detected substantial introgression among different *Rattus* species, particularly evident between *R. norvegicus* and *R. tanezumi*. Strong gene flow signals suggest frequent hybridization events among these species, which may facilitate the acquisition of new environmental adaptability during their expansion into new territories. This study provides a preliminary analysis that serves as a foundation for a more comprehensive investigation into the rapid lineage diversification and adaptive introgression among *Rattus* species.

**Key words:** gene flow, genetic differentiation, invasive species, phylogenetic analysis, *Rattus*.

## 1 Introduction

Human activities and climate change have shifted the ranges of many established invasive species, allowing alien species that would not otherwise have survived to establish and spread (Brauer et al., 2023). The geographical and biological homogenization in the Holocene has occurred as a result of worldwide invasive events (Simberloff, 2013). As the most successful invasive mammals, wild rats in the genus *Rattus* are excellent models for studying adaptive radiations and speciation (Verneau et al., 1998). Previous studies have indicated that *Rattus* originated in Southeast Asia during the Late Miocene (~5.5–7.5 Ma) (Verneau et al., 1998). This genus successfully expanded to New Guinea and Australia (Robins et al., 2014), and is now widespread throughout all continents (Musser & Carleton, 2005). According to the Mammal Diversity Database of the American Society of Mammalogists (https://www.mammaldiversity.org/), which provides the most up-to-date information on global extant mammal species (Burgin et al., 2018), *Rattus* stands out as the most speciose rodent taxon with a total of 71 extant species. Previous studies using cytochrome b (*CYTB*) sequences have investigated the presence of eight *Rattus* species distributed in China (Liu et al., 2018; Xie et al., 2022). However, there is still a lack of genome-wide studies that have explored the phylogenetic relationship and gene flow of this taxon in China and adjacent regions.

Although the majority of *Rattus* species are confined to their natural habitats within their native ranges (Robins et al., 2014), many species of this genus demonstrate a remarkable ability to thrive in disturbed habitats and island ecosystems (Harper & Bunbury, 2015; Puckett et al., 2016). Consequently, a considerable proportion of these species have gained notoriety as invasive pests. The two most widely distributed commensal species, namely *R. rattus* (black rat) and *R. norvegicus* (Norway rat or brown rat), play a pivotal role in the transmission and preservation of zoonotic diseases (Aplin et al., 2011). Additionally, both *R. rattus* and *R. exulans* (Polynesian rat) exhibit ecological invasiveness and have inflicted devastating impacts on native biota (Harper & Bunbury, 2015). While previous studies have predominantly focused on investigating the origins and population demographic history of invasive species (Matisoo-Smith & Robins, 2004; Puckett et al., 2016; Yu et al., 2022), there has been limited exploration into the underlying mechanisms driving the rapid invasion of these species.

The genus *Rattus* represents a classic example of recent and rapid radiations in mammals (Rowe et al., 2011). The divergence between *R. rattus* and its sibling species, *R. tanezumi* (Asian house rat), has been traced back to approximately 0.4 Ma (Robins et al., 2008). *Rattus norvegicus* and *R. nitidus* differentiated as recently as approximately 0.6 Ma (Teng et al., 2017). However, limited ecomorphological differences were presented among species within this genus (Rowe et al., 2011). The diversification of ecological environments in the habitats of *Rattus* species has resulted in the evolution of more environmentally adapted genotypes and accelerated genetic differentiation among species. The heterogeneity of human urban habitat environments has a significant impact on the diversification of rodent species (Puckett et al., 2020). Genomics research can fundamentally provide deeper insights into the evolutionary mechanisms. By analyzing whole-genome data of wild-caught brown rats in northeast China, researchers have found that recent evolution in this species is shaped by declining effective population size (Deinum et al., 2015). Another study assembled a draft genome of the Asian house rat and explored the mechanisms of its northward invasion and the genetic basis underlying plateau adaptation (Chen et al., 2021). A more comprehensive sampling of the genomic data from both widespread-winners and narrow-ranged *Rattus* species in China and the adjacent region is still lacking.

Hybridization enables alien species to acquire locally adapted genotypes, while facilitating the evolution of more adaptive traits in hybrid offspring. This allows them to expand into new habitats that are not occupied by their hybrid parents (Huang et al., 2012). The process of natural hybridization also enhances resilience to climate change and contributes to the evolutionary rescue of species facing threats (Brauer et al., 2023). Recent genome-based studies have provided evidence that hybridization plays a pivotal role in the invasion of the cotton bollworm, an agricultural pest (Valencia-Montoya et al., 2020; Jin et al., 2023), yet its significance in the evolution of rats has been rarely explored. A recent study has found that genes related to chemical communications among introgressed regions appeared to contribute to the population-specific adaptations of the admixed *R. norvegicus* (Teng et al., 2017). However, the interspecific hybridization amongst species within *Rattus* has rarely been investigated in previous studies.

The objective of this study is to investigate the extent of genomic differentiation among morphologically constrained species in *Rattus* and its potential contribution to rapid lineage diversification. Additionally, we aim to examine the occurrence of gene flow between wide-spread invasive and narrow-ranged rat species in China and adjacent regions. To achieve these goals, a genome-wide single nucleotide polymorphism (SNP)-based analysis was conducted on 87 individuals from five *Rattus* species in China and adjacent regions, providing a comprehensive reference dataset for interpreting their phylogenetic relationship and interspecific hybridization.

## 2 Material and Methods

### 2.1 Morphological analyses

To demonstrate morphological differentiation among *Rattus* species, we provided morphological comparison of five species within genus *Rattus* distributed in China, including *R. andamanensis*, *R. nitidus*, *R. norvegicus*, *R. pyctoris*, and *R. tanezumi*. All these specimens were identified by sequencing a mitochondrial genome fragment *CYTB*. The dorsal, ventral, and lateral views of the skin specimens were photographed using an Olympus IM002 camera (Tokyo, Japan), as were the dorsal, ventral, and mandible of the skull specimens (Figs. S1, S2). The body mass (in grams, g), external measurements (EM; in mm) and craniodental measurements (CM; in mm) were integrated using vernier calipers and electronic scales. The mean and standard deviation of the morphological data were calculated for each species. Linear discriminant analysis (LDA) and principal component analysis (PCA) of morphometric linear measurements were performed using PAST version 3.16 (Hammer & Harper, 2001) to examine external and craniodental differences among species (Fig. S3). Collection information and original measurements of these specimens are provided in Tables S1 and S2. Voucher specimens were preserved in the National Zoological Museum, Institute of Zoology, Chinese Academy of Sciences (IOZCAS).

### 2.2 Molecular sampling

We analyzed 91 samples comprising five *Rattus* species ($n = 87$) and two *Niviventer* species ($n = 4$) from China and Russia. Five *Rattus* species were included: *R. norvegicus* ($n = 46$), *R. pyctoris* ($n = 9$), *R. andamanensis* ($n = 8$), *R. nitidus* ($n = 10$), and *R. tanezumi* ($n = 14$), and two *Niviventer* species, *N. fengi* ($n = 2$) and *N. huang* ($n = 2$), were used as the outgroup. Among them, 26 new specimens were collected for whole-genome resequencing. Wild-caught specimens were dissected immediately, and the extracted muscle tissues were stored in 95% ethanol at −80°C. Four specimens of the genus *Niviventer* were obtained from a previous study (Wu et al., 2023). The specimens of rats used in this study are preserved in IOZCAS and the Zoological Institute, Russian Academy of Sciences (ZIN). *Rattus norvegicus* were sampled from northern to southern China and Russian adjacent regions, thus providing a broad representation of *R. norvegicus* diversity across its geographic range in China and adjacent regions. Other species were sampled within their

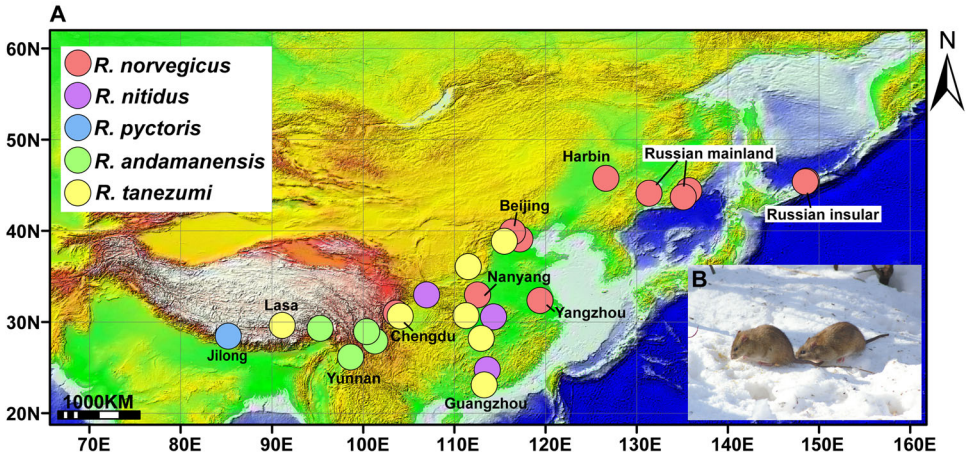


**Fig. 1.** Geographical distribution of *Rattus* samples used in the present study. **A,** Sample locations of molecular voucher specimens for whole-genome sequencing. **B,** *Rattus norvegicus*, park in Moscow, Russia, 2013. Credit: Sergei V. Kruskop.

natural habitat. The sampling sites for *Rattus* species were mapped on a topography map (Fig. 1). Detailed information for localities of these specimens is provided in Table S3.

### 2.3 DNA extraction and sequencing

Genomic DNA samples were extracted from muscle tissue using the Qiagen DNeasy Blood and Tissue Kit (Qiagen China, Shanghai, China). The extracted genomic DNA was sequenced by the Beijing Genomics Institute (Beijing, China). The quality and integrity of the extracted DNA were checked by measuring the A260/A280 ratio using a NanoDrop ND-2000 spectrophotometer (Thermo Fisher Scientific, Carlsbad, California, USA) and by agarose gel electrophoresis. DNBSEQ whole genome sequencing libraries with insert size of approximately 350 bp were prepared and sequenced on DNBSEQ T7 platform with 150 bp paired-end reads. Raw reads were filtered using fastp version 0.20.1 (Chen et al., 2018) to filter out adapter sequences as well as low-quality reads. FastQC version 0.11.9 (Schmieder & Edwards, 2011) was used to assess the quality of clean reads.

### 2.4 Single nucleotide polymorphism calling and filtering

We mapped the clean reads of all sequenced individuals to the *R. norvegicus* reference genome (GCF_015227675.2_mRatBN7.2 from the National Center for Biotechnology Information [NCBI]) by BWA version 0.7.17 (Li & Durbin, 2009). In addition to new data generated in this study, we obtained SRA data of *R. norvegicus*, *R. nitidus*, and *R. tanezumi* from public databases, including a total of 61 samples obtained from the NCBI and National Genomics Data Center databases. The mapping files were then sorted and filtered by removing polymerase chain reaction duplicates with SAMtools version 1.12 (Li et al., 2009). After mapping, SNP calling was carried out using BCFtools version 1.12 (Li, 2011). VCFtools version 0.1.16 (Danecek et al., 2011) was used to filter and obtain high-quality SNPs for subsequent analysis. The following filtering strategy was used: (i) genotype quality >30; (ii) minimum sequencing depth = 5, maximum sequencing depth = 50; (iii) missing rates <30%; and (iv) minor allele frequency >0.05. Data size and accession numbers of data newly generated in this study are given in Table S4. In addition, the accession numbers of additional SRA data are listed in Table S5.

### 2.5 Phylogenetic reconstruction using the mitochondrial genome

We established a dataset of 263 individuals to reconstruct the phylogeny of *Rattus* species: the mitochondrial genome sequences (MTGs) of 26 individuals that were newly sequenced in the present study and 211 individuals obtained from NCBI plus those of *Niviventer* species available from a previous study (Wu et al., 2023), and the *CYTB* for 26 individuals of *R. losea* available from GenBank. *Niviventer* species were used as the outgroup in the phylogenetic reconstruction.

GetOrganelle-master (Jin et al., 2020) was used to assemble the MTGs from the clean data. The MTGs from NCBI and those generated in the current study were annotated by the MITOS online server (Bernt et al., 2013). Thirteen mitochondrial protein-coding genes extracted from MTGs were aligned using Muscle version 3.8.31 (Edgar, 2004) and concatenated together. We performed a maximum likelihood (ML) analysis using IQ-TREE version 1.6.12 (Minh et al., 2020). The mutation model we used was GTR + F + I + G4. The ML tree was visualized and edited using iTOL (https://itol.embl.de/) (Letunic & Bork, 2021). Mitochondrial genomes obtained in this study were submitted to the China National GeneBank database with accession numbers N_001486735 to N_001486760, and detailed information for data newly assembled in phylogenetic reconstruction is given in Table S6. Moreover, the accession numbers of samples from NCBI used for phylogenetic analysis are given in Table S7.

### 2.6 Population structure analysis of the nuclear genome

Phylogenetic trees were constructed based on high-quality SNPs using the ML and neighbor-joining (NJ) approaches, with the genus *Niviventer* as the outgroup. The ML tree was inferred using IQ-TREE version 1.6.12 (Minh et al., 2020) with 1000 bootstraps. The optimal mutation model and tree were inferred using the "-m MFP" parameter. TVM + F + R3 was

identified as the fittest model. Next, the NJ tree was constructed by means of FastMe version 2.0 (Lefort et al., 2015), with the nucleotide *P*-distance matrix using VCF2Dis. The two trees were visualized and edited using iTOL (https://itol.embl.de/) (Letunic & Bork, 2021). Genetic structure was assessed using PCA with whole-genome SNPs for all 87 individuals using PLINK version 1.90b6.21 (Purcell et al., 2007). ADMIXTURE version 1.3.0 (Alexander & Lange, 2011) was also used to analyze the population structure. First, the *Niviventer* species were removed from the SNPs dataset. To mitigate the effects of linkage disequilibrium (LD) on genetic structure, we pruned the markers using the "--indep-pairwise 50 10 0.2" option of PLINK version 1.90b6.21 (Purcell et al., 2007). After filtering, 8 613 990 SNPs remained for analysis. The number of assumed genetic clusters (*K*) ranged from two to nine.

### 2.7 Genetic distance analysis

Sequence genetic distances were calculated for MTGs using MEGA11 (Tamura et al., 2021) under the Kimura two-parameter model (Kimura, 1980). The individuals were grouped using the "Select Taxa and Group" option in the "DATA" module. The genetic distance was then calculated using the "Compute Between Group Mean Distance" option in the "DISTANCE" module. Then, the Kimura two-parameter model was chosen and the bootstrap value was set to 1000. In addition, population-differentiation statistics (fixation index [$F_{st}$]) (Weir & Cockerham, 1984) of SNPs were calculated using VCFtools version 0.1.16 (Danecek et al., 2011) with a 100 kb nonoverlapping sliding window. Pairwise comparisons of the $F_{st}$ between *Rattus* species were calculated based on the average value of all sliding windows.

### 2.8 Overall gene flow analysis

The SNP-based *D* statistics (also known as ABBA-BABA) were computed to assess gene flow among a subset of taxa. According to the species tree topology constructed by using SNPs, the *Niviventer* spp. were set as the outgroup, and the Dtrios module in the Dsuite (Malinsky et al., 2021) was used to calculate all possible overall *D*-statistic (Durand et al., 2011) and f4-ratios (Patterson et al., 2012) in five *Rattus* species. The f-branch module was run in Dsuite to map the strength of gene flow among species, with the species tree and the output of the Dsuite Dtrios analysis as input (Malinsky et al., 2018). The results were visualized as heatmaps using "plot_d.rb", "plot_f4ratio.rb", and "dtools.py".

TreeMix (Pickrell & Pritchard, 2012) was used to infer the most likely population topology while considering potential gene flow between the branches. We pruned the filtered high-quality SNPs in high LD. In addition, sites with missing values were removed from the analyses. The ML tree of populations was estimated using the genome-wide allele frequency data, with *Niviventer* spp. being used as the outgroup. We conducted 10 repeats for each *m* value (migration edge) from 0 to 5 and used the R package OptM (Fitak, 2021) to evaluate the optimal number of migration edges. The output of TreeMix was treated as the input file of OptM. The scripts of plotting_funcs. R was used to plot the results.

## 3 Results

### 3.1 Morphological differentiation

Measurements of external and craniodental data for *Rattus* species have been summarized in Table S8, with the mean ± standard deviation indicating the variation within species. Despite the limited morphological differences observed among species, it is possible to identify them based on specific characteristics. For example, *R. norvegicus* has shorter ears and tail, *R. andamanensis* has a distinct dorsal and ventral color boundary and a pure white belly, and the ventral surface of *R. tanezumi* is tawny (Fig. S1). The skull of *R. norvegicus* is characterized by the temporal crests being almost parallel, with the right and left temporal crests extending backward and parallel without extending outward (Fig. S2).

In the PCA analysis of CM, the first two principal components explained 67.01% and 7.57% of the total variance, respectively (Fig. S3A). The species exhibit considerable overlap, suggesting that differentiation in skull morphology is not remarkable (Fig. S3A). The first two axes of the LDA analysis of EMs explained 76.4% and 21.6% of the variance, respectively, indicating a high degree of overlap among species (Fig. S3B). This suggests that divergence in external morphology was also not significant. Additionally, the LDA analysis of CM revealed a little more pronounced differentiation among species (Fig. S3C).

### 3.2 Genome-scale sequencing

This study involved the whole genome resequencing of 26 individuals from three *Rattus* species. Approximately 1030 Gb of 150 bp paired-end reads were obtained, with an average sequencing depth of 17.28*x* per individual. The average Q20 and Q30 were above 97% and 92%, respectively. Twenty-six individuals that were newly sequenced in the present study, four individuals of the genus *Niviventer* obtained from a published study, and 61 individuals of the genus *Rattus* downloaded from public databases comprised a dataset of 91 individuals. After performing quality control and filtering, the paired-end clean reads of 91 individuals were aligned to the *R. norvegicus* reference genome, obtaining a total of 285 654 586 initial SNPs, which were filtered using VCFtools version 0.1.16 (Danecek et al., 2011) to obtain high-quality SNPs of 33 036 574 for subsequent analyses.

### 3.3 Phylogenetic reconstruction of the mitochondrial genome

Using IQ-TREE version 1.6.12 (Minh et al., 2020), we performed the phylogenetic reconstruction of the MTGs dataset of 263 individuals to construct an ML tree. The results showed species of the genus *Rattus* were classified into two clades, Eurasia and Australia, with reliable confidence (bootstrap value = 100); all *Rattus* spp. distributed in China were located in the Eurasia clade (Fig. 2). In addition, *R. norvegicus* is most closely related to *R. nitidus*. *Rattus nitidus* diverged to two clades that include Xizang and nominotypical subspecies of this species. *Rattus rattus* is a sibling species to *R. tanezumi*.

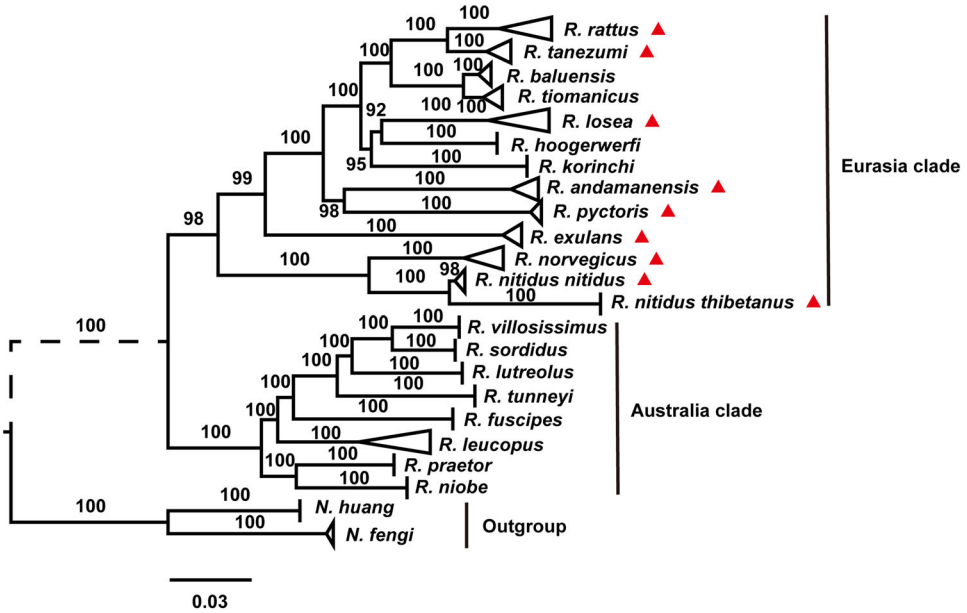


**Fig. 2.** Phylogenetic tree of *Rattus* species, constructed based on 13 protein-coding sequences of mitochondrial genome sequences. Species distributed in China are indicated by red triangles.

### 3.4 Genomic differentiation inferred using nuclear genome

Phylogenetic trees were constructed using the ML and NJ approaches based on high-quality SNPs. The NJ tree and ML tree topology showed similarities, with the outgroup *Niviventer* spp. rooting the tree, and the *Rattus* species yielding five well-separated branches (Figs. 3A, S4). *Rattus norvegicus* and its sibling species, *R. nitidus*, were clustered in one large clade, whereas *R. tanezumi*, *R. andamanensis*, and *R. pyctoris* formed another monophyletic clade. The ML tree revealed the divergence of *R. norvegicus*, with the initial split observed among samples from Yangzhou, while the populations from the Russian Far East and Harbin exhibited the most recent divergence (Fig. 3A). This result indicated a tendency towards expansion from south to north of *R. norvegicus*, consistent with previous studies (Song et al., 2014).

We conducted PCA on five *Rattus* species by using SNPs. The PCA results revealed that *R. norvegicus* was genetically distinguished from the other species, while the remaining species formed a cluster with the mosaic distribution (Fig. 3B). The *R. norvegicus* populations in China and Russia have diverged significantly. Samples from the Russian Far East include samples from Iturup Island (approximately 147–148°E) and the mainland Far East (approximately 131–135°E), of which the mainland population was more similar to the Chinese population. PCA of the remaining four species showed that *R. nitidus* and *R. tanezumi* were further separated, while *R. andamanensis* clustered with *R. pyctoris*, suggesting a close relationship between these two species.

Admixture version 1.3.0 (Alexander & Lange, 2011) was used to infer the population structure. In addition, the number of ancestral composition *K* was predefined from 2–9 (Fig. 3C). For $K = 2$, *R. norvegicus* distinguished itself from other species. For $K = 6$, the minimum coefficient of variation was 0.263, indicating the best-supported cluster. *Rattus norvegicus* populations were divided into three groups, the Russian Far East insular population, Russian Far East mainland-Chinese population, and Nanyang population. *Rattus andamanensis* showed a high genetic affinity with *R. pyctoris*, which was also consistent with the result of PCA. For $K = 9$, *R. tanezumi* was divided into two distinct groups, one group from low-altitude areas of China and another from Lasa, Xizang, China.

### 3.5 Genetic distance among species

To measure the degree of genetic differentiation among *Rattus* species, we calculated pairwise genetic distances based on the 13 mitochondrial protein-coding gene sequences using the K2-P model in MEGA11 (Tamura et al., 2021). The K2-P distances among the *Rattus* species distributed in China ranged from 0.040 to 0.136, with an average distance of 0.109, indicating a significant degree of genetic differentiation among them. The smallest distance occurred between *R. rattus* and *R. tanezumi*, followed by *R. norvegicus* and *R. nitidus* with 0.066, verifying the sibling species relationship between them. The largest distance was between *R. losea* and *R. nitidus* (Table 1).

We also calculated pairwise $F_{st}$ between *Rattus* species using the SNP dataset (Table 2). The pairwise comparisons of *Fst* ranged from 0.123 to 0.242. This suggests that the *Rattus* species have undergone a moderate level of differentiation. The species with the smallest differentiation were clustered between *R. norvegicus* and its sibling species, *R. nitidus*. *Rattus norvegicus* had lower differentiation indexes with all other species, indicating some degree of genetic affinity.

### 3.6 Overall gene flow analyses

Admixture was also used to assess ancestral mixture proportion among *Rattus* species. *R. norvegicus* shows evidence of gene flow with other species. In the *R. norvegicus* block of admixture results, there was the presence

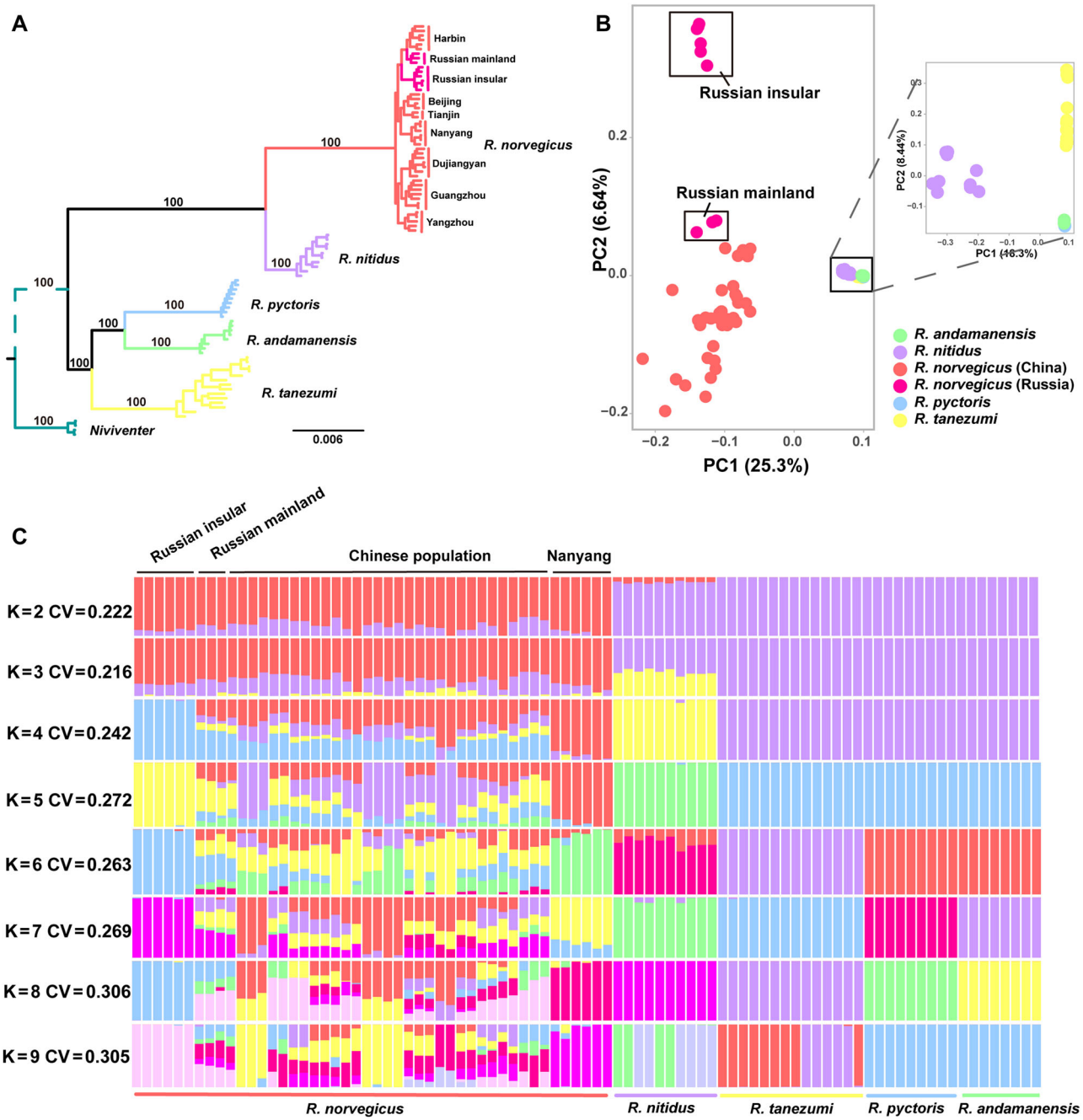


**Fig. 3.** Genetic structure among *Rattus* species. **A,** A maximum likelihood tree was inferred using single nucleotide polymorphisms. **B,** Genetic structure inferred using principal component analysis. **C,** Ancestral composition inferred using ADMIXTURE. CV, coefficient of variation; K, assumed genetic clusters; PC, principal component.

of the mixture of multiple ancestral components (Fig. 3C). The Russian population, located at Iturup Island within its range, was relatively homogeneous. TreeMix (Pickrell & Pritchard, 2012) accurately described the direction and degree of introgression. The ML species tree for all species was displayed by TreeMix (Fig. S5). The OptM results indicated that $m = 4$ was the most statistically parsimonious (Fig. S6), with *R. tanezumi* introgression to *R. norvegicus* and *R. andamanensis*, *R. nitidus* introgression to *R. pyctoris*, and *R. andamanensis* introgression to *R. nitidus* (Fig. 4A). To further explore gene flow across all *Rattus* species, we performed the *D*-statistic, f4-ratio, and f-branch in Dsuite (Malinsky et al., 2021), which identified significant introgression signals among three species pairs (Figs. 4B–4D; Table S9). Overall, we identified strong gene flow between *R. norvegicus* and *R. tanezumi*, *R. nitidus* and *R. pyctoris*, and *R. nitidus* and *R. andamanensis*, with the composition of *R. norvegicus* and *R. tanezumi* showing the strongest signal.

**Table 1** Estimates of evolutionary divergence over mitochondrial protein-coding sequence pairs between *Rattus* species

| | RA | RB | RE | RF | RH | RK | RLE | RLO | RLU | RNI | RNIT | RNO | RPR | RPY | RR | RSO | RTA | RTI | RTU |
|---|---|---|---|---|---|---|---|---|---|---|---|---|---|---|---|---|---|---|---|
| **RB** | 0.0921 | | | | | | | | | | | | | | | | | | |
| **RE** | 0.1190 | 0.1123 | | | | | | | | | | | | | | | | | |
| **RF** | 0.1368 | 0.1321 | 0.1386 | | | | | | | | | | | | | | | | |
| **RH** | 0.0978 | 0.0753 | 0.1127 | 0.1330 | | | | | | | | | | | | | | | |
| **RK** | 0.1033 | 0.0815 | 0.1175 | 0.1365 | 0.0816 | | | | | | | | | | | | | | |
| **RLE** | 0.1362 | 0.1300 | 0.1334 | 0.0874 | 0.1325 | 0.1334 | | | | | | | | | | | | | |
| **RLO** | 0.0982 | 0.0772 | 0.1043 | 0.1309 | 0.0728 | 0.0886 | 0.1199 | | | | | | | | | | | | |
| **RLU** | 0.1335 | 0.1296 | 0.1393 | 0.0888 | 0.1356 | 0.1364 | 0.0871 | 0.1239 | | | | | | | | | | | |
| **RNI** | 0.1270 | 0.1231 | 0.1307 | 0.0886 | 0.1263 | 0.1305 | 0.0862 | 0.1175 | 0.0929 | | | | | | | | | | |
| **RNIT** | 0.1234 | 0.1224 | 0.1261 | 0.1322 | 0.1231 | 0.1277 | 0.1262 | 0.1364 | 0.1332 | 0.1281 | | | | | | | | | |
| **RNO** | 0.1262 | 0.1215 | 0.1231 | 0.1275 | 0.1217 | 0.1255 | 0.1221 | 0.1286 | 0.1294 | 0.1246 | 0.0658 | | | | | | | | |
| **RPR** | 0.1282 | 0.1222 | 0.1326 | 0.0850 | 0.1266 | 0.1293 | 0.0820 | 0.1243 | 0.0896 | 0.0637 | 0.1274 | 0.1232 | | | | | | | |
| **RPY** | 0.1018 | 0.0972 | 0.1249 | 0.1370 | 0.0997 | 0.1024 | 0.1343 | 0.1014 | 0.1361 | 0.1288 | 0.1272 | 0.1238 | 0.1325 | | | | | | |
| **RR** | 0.0997 | 0.0646 | 0.1171 | 0.1340 | 0.0795 | 0.0853 | 0.1323 | 0.0700 | 0.1342 | 0.1247 | 0.1265 | 0.1257 | 0.1264 | 0.1000 | | | | | |
| **RSO** | 0.1330 | 0.1251 | 0.1343 | 0.0890 | 0.1324 | 0.1338 | 0.0882 | 0.1277 | 0.0643 | 0.0860 | 0.1317 | 0.1271 | 0.0834 | 0.1328 | 0.1290 | | | | |
| **RTA** | 0.0984 | 0.0636 | 0.1151 | 0.1325 | 0.0790 | 0.0827 | 0.1298 | 0.0774 | 0.1323 | 0.1237 | 0.1255 | 0.1275 | 0.1244 | 0.0990 | 0.0397 | 0.1285 | | | |
| **RTI** | 0.0958 | 0.0208 | 0.1128 | 0.1361 | 0.0767 | 0.0838 | 0.1312 | 0.0761 | 0.1316 | 0.1243 | 0.1229 | 0.1217 | 0.1238 | 0.0996 | 0.0664 | 0.1259 | 0.0660 | | |
| **RTU** | 0.1350 | 0.1270 | 0.1388 | 0.0935 | 0.1340 | 0.1388 | 0.0929 | 0.1480 | 0.0761 | 0.0944 | 0.1331 | 0.1277 | 0.0916 | 0.1366 | 0.1318 | 0.0727 | 0.1320 | 0.1285 | |
| **RVI** | 0.1345 | 0.1272 | 0.1331 | 0.0906 | 0.1335 | 0.1359 | 0.0882 | 0.1320 | 0.0645 | 0.0886 | 0.1331 | 0.1266 | 0.0859 | 0.1379 | 0.1315 | 0.0421 | 0.1294 | 0.1288 | 0.0725 |

Abbreviations: RA, *R. andamanensis*; RB, *R. baluensis*; RE, *R. exulans*; RF, *R. fuscipes*; RH, *R. hoogerwerfi*; RK, *R. korinch*; RLE, *R. leucopus*; RLO, *R. losea*; RLU, *R. lutreolus*; RNI, *R. niobe*; RNIT, *R. nitidus*; RNO, *R. norvegicus*; RPR, *R. praetor*; RPY, *R. pyctoris*; RR, *R. rattus*; RSO, *R. sordidus*; RTA, *R. tanezumi*; RTI, *R. tiomanicus*; RTU, *R. tunneyi*; RVI, *R. villosissimus*.

**Table 2** Pairwise comparisons of fixation index ($F_{st}$) using single nucleotide polymorphisms between *Rattus* species

| | *R. andamanensis* | *R. nitidus* | *R. norvegicus* | *R. pyctoris* |
|---|---|---|---|---|
| *R. nitidus* | 0.224 | | | |
| *R. norvegicus* | 0.137 | 0.123 | | |
| *R. pyctoris* | 0.235 | 0.242 | 0.144 | |
| *R. tanezumi* | 0.185 | 0.228 | 0.160 | 0.211 |

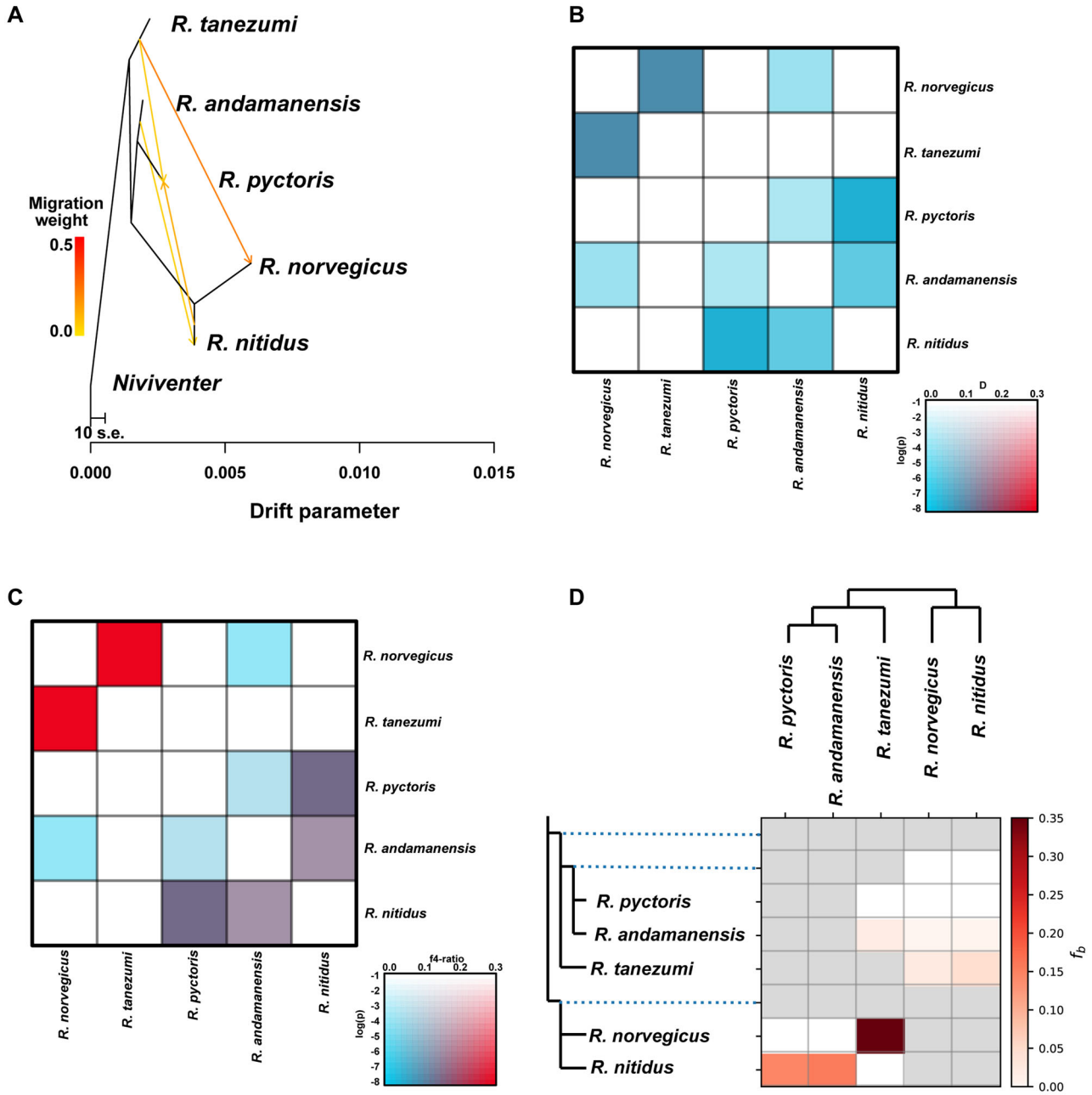


**Fig. 4.** Hybridization among *Rattus* species. **A,** Gene flow detected using TreeMix. **B,** Gene flow determined using *D* statistics in Dsuite. **C,** Gene flow determined using the F4-ratio. **D,** Gene flow determined using the f-branch method.

# 4 Discussion

### 4.1 High genome-level genetic differentiation among *Rattus* species

The evidence of morphological similarity suggests limited morphological differences among *Rattus* species (Figs. S1–S3), which is consistent with a previous study (Robins et al., 2014). On the contrary, we detected significant genome-level genetic differentiation among *Rattus* species. The analyses of genetic distance can also be utilized for quantifying species affinities, tracing gene flow patterns, and elucidating the evolutionary trajectory (Shirk et al., 2017; Mugula et al., 2023). In our study, the K2-P distances based on 13 mitochondrial protein-coding gene sequences indicate moderate differentiation among *Rattus* species distributed in China. Combined with the $F_{st}$ results, we hypothesize that genomic differentiation might play a more important role than the morphological diversification in *Rattus*. High genetic affinities were detected between *R. rattus* and *R. tanezumi*, *R. norvegicus*, and *R. nitidus*, which are consistent with their sibling species relationship. Moreover, in the $F_{st}$ test, *R. norvegicus* showed lower differentiation indexes with all other species, implying the impact of potential gene flow.

Meanwhile, in the phylogenetic reconstruction of the mitochondrial genome, the genus *Rattus* is geographically compartmentalized into two distinct clades, Eurasian and Australian. These clades represent discrete biogeographic regions, suggesting that different branches of *Rattus* species have undergone adaptive evolution in response to varying geographic and climatic conditions. Phylogenetic analyses also revealed a well-branched structure with high statistical support for all *Rattus* spp., which may be influenced by geographical isolation and historical long-distance migrations (Aplin et al., 2011). These findings imply that as invasive rats continue to expand their range, the diversification of ecological environments has driven environmentally-driven evolutionary processes, resulting in accelerated genetic differentiation among species. Further investigations are warranted to identify highly differentiated genes or regional signals through functional analysis in future studies.

*Rattus norvegicus* and *R. tanezumi* are both invasive species showing a wide geographic distribution, with the former having a global presence while the latter is currently expanding its range from southern Asia to northern China (Chen et al., 2021). Our samples were collected from diverse ecosystems, including the Qinghai–Tibet Plateau (QHTP), spanning from southern to northern China, as well as the Russian periphery of northeast Asia. The uplift of QHTP and the distinct climatic ecologies of the continent and islands may have facilitated divergence among species in *Rattus*, and the speciation of *R. pyctoris* and *R. andamanensis*, potentially representing adaptive differentiation in this genus (Favre et al., 2015). The extensive distribution of *R. norvegicus* has been attributed to differentiation among its geographically diverse populations and human-aided range expansion (Puckett et al., 2020). In our study, island populations in the Russian Far East constitute isolated, pure, and harmonious populations that align with long-term geographic isolation within island ecosystems. Similarly, *R. tanezumi* and *R. nitidus* from Xizang exhibit notable differentiation compared to those sampled in low-altitude areas of China. The mountainous region surrounding QHTP serves as a cradle for biodiversity, where its unique climate has shaped highly specialized species (He et al., 2020).

### 4.2 Strong gene flow signals among *Rattus* species

Hybridization contributes to the adaptive evolution and genetic rescue of species, thereby improving their capacity to adapt and spread (Prentis et al., 2008; Ralls et al., 2020). In this study, ADMIXTURE results revealed that the invasive species, *R. norvegicus*, has potential gene flow with native species. Dsuite and TreeMix analyses detected substantial introgression signals between different *Rattus* species. Complex gene flow may modify the gene pools of species and contribute to their evolutionary innovation (Tigano & Friesen, 2016; Greve & Pertierra, 2022). It is possible that hybridization with allied species has facilitated the northward expansion of the rat species as well as high-altitude adaptation. Among these hybridization events, the strongest introgressive signal was detected between *R. norvegicus* and *R. tanezumi*. In our study, there are multiple overlaps in the ranges of the widely distributed *R. norvegicus* and *R. tanezumi*, which may have facilitated gene flow between these two species. Previous studies have shown that chronic interspecific interactions may have contributed to the invasion of *R. tanezumi*, which expanded northward in China into the range of *R. norvegicus* by odor suppression in natural sympatric habitats (Guo et al., 2017). This advantage may have enabled *R. tanezumi* to compete with the much larger *R. norvegicus*. Meanwhile, the study found that females of *R. tanezumi* are more likely to be attracted by the male urine of *R. norvegicus* over those of their own males (Guo et al., 2017). The occurrence of this phenomenon coincides with the identification of significant hybridization signals between *R. tanezumi* and *R. norvegicus*. We hypothesize that through hybridization with *R. norvegicus*, *R. tanezumi* may have also acquired advantageous alleles that facilitate rapid adaptation to changing environments, greater competitiveness, and expansion of its survival range. For instance, it has been reported that anticoagulant resistance and chemical communication-associated genes obtained through hybridization contribute to the enhanced adaptation and rapid expansion of invasive rodents (Song et al., 2011; Teng et al., 2017). However, the genetic background and genomic effects of high-level introgression remain unclear and are worthy of further study with more extensive sampling.

Additionally, the *R. norvegicus* insular population from the Russian Far East was relatively pure, whereas the mainland population was more closely related to the populations from China, suggesting that hybridization of *R. norvegicus* from China and other native species might have occurred later, and that there was a process of two dispersals of this species to the Russian Far East, the second of which may be a post-hybridization dispersal.

# 5 Outlook

The contribution of genomic variation and expression differences in the adaptive advantages of *Rattus* species expansion into diverse novel environments remains to be elucidated. To achieve this, it is necessary to integrate

additional genomic and transcriptomic data. The application of multiple analyses at both the genome and transcriptome levels is expected to facilitate a more comprehensive understanding of the genetic nature underlying species differentiation and adaptive evolution.

The gene flow analyses revealed a significant exchange of genetic material between *R. norvegicus* and *R. tanezumi*, indicating the occurrence of interspecies hybridization. Further investigation is required to precisely identify the specific loci involved in this introgression and elucidate the functional implications of these genes. Subsequently, we will explore the role of hybridization events in facilitating species invasion success and enhancing competitive advantage acquisition.

We will delve into the origins, proliferation, and evolutionary dynamics of genus *Rattus*. A broader range of samples and fossil data will be obtained. Subsequently, ancient DNA analysis and molecular clock modeling analysis should be undertaken to resolve the origin and dispersal controversies of species within the genus *Rattus*, especially *R. norvegicus*.

## Acknowledgements

This work was supported by the Guangdong Provincial Key R&D Program (2022B1111040001), the Survey of Wildlife Resources in Key Areas of Xizang (Phase II, ZL202303601), the Second Tibetan Plateau Scientific Expedition and Research Program (2019QZKK0402), the National Natural Science Foundation of China (32170426), and the Ministry of Science and Higher Education of the Russian Federation (075-15-2021-1069).

## Data Availability Statement

The datasets containing the accession numbers for *Rattus* generated in this study are available as supplemental information. Original sequence reads of genome data are available at the China National GeneBank (Accession number CNP0005706), and the assembled sequence of mitochondrial data are available at the China National GeneBank DataBase (Accession number N_001486735-N_001486760).

## References

Alexander DH, Lange K. 2011. Enhancements to the admixture algorithm for individual ancestry estimation. *BMC Bioinformatics* 12: 246.

Aplin KP, Suzuki H, Chinen AA, Chesser RT, Ten Have J, Donnellan SC, Austin J, Frost A, Gonzalez JP, Herbreteau V, Catzeflis F, Soubrier J, Fang YP, Robins J, Matisoo-Smith E, Bastos ADS, Maryanto I, Sinaga MH, Denys C, Van Den Bussche RA, Conroy C, Rowe K, Cooper A. 2011. Multiple geographic origins of commensalism and complex dispersal history of black rats. *PLoS One* 6: e26357.

Bernt M, Donath A, Jühling F, Externbrink F, Florentz C, Fritzsch G, Pütz J, Middendorf M, Stadler PF. 2013. Mitos: Improved de novo metazoan mitochondrial genome annotation. *Molecular Phylogenetics and Evolution* 69: 313–319.

Brauer CJ, Sandoval-Castillo J, Gates K, Hammer MP, Unmack PJ, Bernatchez L, Beheregaray LB. 2023. Natural hybridization reduces vulnerability to climate change. *Nature Climate Change* 13: 282–289.

Burgin CJ, Colella JP, Kahn PL, Upham NS. 2018. How many species of mammals are there? *Journal of Mammalogy* 99: 1–14.

Chen SF, Zhou YQ, Chen YR, Gu J. 2018. Fastp: An ultra-fast all-in-one fastq preprocessor. *Bioinformatics* 34: i884–i890.

Chen Y, Hou GM, Jing MD, Teng HJ, Liu QS, Yang XG, Wang Y, Qu JP, Shi CM, Lu L, Zhang JX, Zhang YH. 2021. Genomic analysis unveils mechanisms of northward invasion and signatures of plateau adaptation in the Asian house rat. *Molecular Ecology* 30: 6596–6610.

Danecek P, Auton A, Abecasis G, Albers CA, Banks E, DePristo MA, Handsaker RE, Lunter G, Marth GT, Sherry ST, McVean G, Durbin R. 2011. The variant call format and vcftools. *Bioinformatics* 27: 2156–2158.

Deinum EE, Halligan DL, Ness RW, Zhang YH, Cong L, Zhang JX, Keightley PD. 2015. Recent evolution in *Rattus norvegicus* is shaped by declining effective population size. *Molecular Biology and Evolution* 32: 2547–2558.

Durand EY, Patterson N, Reich D, Slatkin M. 2011. Testing for ancient admixture between closely related populations. *Molecular Biology and Evolution* 28: 2239–2252.

Edgar RC. 2004. Muscle: Multiple sequence alignment with high accuracy and high throughput. *Nucleic Acids Research* 32: 1792–1797.

Favre A, Päckert M, Pauls SU, Jähnig SC, Uhl D, Michalak I, Muellner-Riehl AN. 2015. The role of the uplift of the Qinghai-Tibetan Plateau for the evolution of Tibetan biotas. *Biological Reviews* 90: 236–253.

Fitak RR. 2021. OptM: Estimating the optimal number of migration edges on population trees using Treemix. *Biology Methods & Protocols* 6: 017.

Greve M, Pertierra LR. 2022. Opportunities for studying propagule pressure using gene flow reveal its role in accelerating biological invasions. *Molecular Ecology* 31: 1609–1611.

Guo HL, Teng HJ, Zhang JH, Zhang JX, Zhang YH. 2017. Asian house rats may facilitate their invasive success through suppressing brown rats in chronic interaction. *Frontiers in Zoology* 14: 20.

Hammer Ø, Harper DA. 2001. PAST: Paleontological statistics software package for educaton and data anlysis. *Palaeontologia Electronica* 4: 1.

Harper GA, Bunbury N. 2015. Invasive rats on tropical islands: Their population biology and impacts on native species. *Global Ecology and Conservation* 3: 607–627.

He JK, Lin SL, Li JT, Yu JH, Jiang HS. 2020. Evolutionary history of zoogeographical regions surrounding the Tibetan Plateau. *Communications Biology* 3: 415.

Huang DC, Zhang RZ, Kim KC, Suarez AV. 2012. Spatial pattern and determinants of the first detection locations of invasive alien species in Mainland China. *PLoS One* 7: e31734.

Jin JJ, Yu WB, Yang JB, Song Y, dePamphilis CW, Yi TS, Li DZ. 2020. Getorganelle: A fast and versatile toolkit for accurate de novo assembly of organelle genomes. *Genome Biology* 21: 241.

Jin MH, North HL, Peng Y, Liu HW, Liu B, Pan RQ, Zhou Y, Zheng WG, Liu KY, Yang B, Zhang L, Xu Q, Elfekih S, Valencia-Montoya WA, Walsh T, Cui P, Zhou YF, Wilson K, Jiggins C, Wu KM, Xiao YT. 2023. Adaptive evolution to the natural and anthropogenic environment in a global invasive crop pest, the cotton bollworm. *The Innovation* 4: 100454.

Kimura M. 1980. A simple method for estimating evolutionary rates of base substitutions through comparative studies of nucleotide sequences. *Journal of Molecular Evolution* 16: 111–120.

Lefort V, Desper R, Gascuel O. 2015. Fastme 2.0: A comprehensive, accurate, and fast distance-based phylogeny inference program. *Molecular Biology and Evolution* 32: 2798–2800.

Letunic I, Bork P. 2021. Interactive Tree Of Life (iTOL) v5: An online tool for phylogenetic tree display and annotation. *Nucleic Acids Research* 49: W293–W296.

Li H. 2011. A statistical framework for SNP calling, mutation discovery, association mapping and population genetical parameter estimation from sequencing data. *Bioinformatics* 27: 2987–2993.

Li H, Durbin R. 2009. Fast and accurate short read alignment with Burrows-Wheeler transform. *Bioinformatics* 25: 1754–1760.

Li H, Handsaker B, Wysoker A, Fennell T, Ruan J, Homer N, Marth G, Abecasis G, Durbin R. 2009. The sequence alignment/Map format and SAMtools. *Bioinformatics* 25: 2078–2079.

Liu SY, He K, Chen SD, Jin W, Murphy RW, Tang MK, Liao R, Li FJ. 2018. How many species of *Apodemus* and *Rattus* occur in China? A survey based on mitochondrial cyt b and morphological analyses. *Zoological Research* 39: 309–320.

Malinsky M, Matschiner M, Svardal H. 2021. Dsuite—Fast D-statistics and related admixture evidence from VCF files. *Molecular Ecology Resources* 21: 584–595.

Malinsky M, Svardal H, Tyers AM, Miska EA, Genner MJ, Turner GF, Durbin R. 2018. Whole-genome sequences of Malawi cichlids reveal multiple radiations interconnected by gene flow. *Nature Ecology & Evolution* 2: 1940–1955.

Matisoo-Smith E, Robins JH. 2004. Origins and dispersals of Pacific peoples: Evidence from mtDNA phylogenies of the Pacific rat. *Proceedings of the National Academy of Sciences* 101: 9167–9172.

Minh BQ, Schmidt HA, Chernomor O, Schrempf D, Woodhams MD, von Haeseler A, Lanfear R. 2020. IQ-TREE 2: New models and efficient methods for phylogenetic inference in the genomic era. *Molecular Biology and Evolution* 37: 1530–1534.

Mugula BB, Omondi SF, Curto M, Kiboi SK, Kanya JI, Egeru A, Okullo P, Meimberg H. 2023. Microsatellites reveal divergence in population genetic diversity, and structure of *Osyris lanceolata* (Santalaceae) in Uganda and Kenya. *BMC Ecology and Evolution* 23: 73.

Musser G, Carleton M. 2005. *Superfamily Muroidea. Mammal species of the world: A taxonomic and geographic reference*. Baltimore, Maryland, USA: The Johns Hopkins University Press. 894–1531.

Patterson N, Moorjani P, Luo Y, Mallick S, Rohland N, Zhan Y, Genschoreck T, Webster T, Reich D. 2012. Ancient admixture in human history. *Genetics* 192: 1065–1093.

Pickrell JK, Pritchard JK. 2012. Inference of population splits and mixtures from genome-wide allele frequency data. *PLoS Genetics* 8: e1002967.

Prentis PJ, Wilson JRU, Dormontt EE, Richardson DM, Lowe AJ. 2008. Adaptive evolution in invasive species. *Trends in Plant Science* 13: 288–294.

Puckett EE, Orton D, Munshi-South J. 2020. Commensal rats and humans: Integrating rodent phylogeography and zooarchaeology to highlight connections between human societies. *BioEssays* 42: 1900160.

Puckett EE, Park J, Combs M, Blum MJ, Bryant JE, Caccone A, Costa F, Deinum EE, Esther A, Himsworth CG, Keightley PD, Ko A, Lundkvist Å, McElhinney LM, Morand S, Robins J, Russell J, Strand TM, Suarez O, Yon L, Munshi-South J. 2016. Global population divergence and admixture of the brown rat (*Rattus norvegicus*). *Proceedings of the Royal Society B: Biological Sciences* 283: 20161762.

Purcell S, Neale B, Todd-Brown K, Thomas L, Ferreira MAR, Bender D, Maller J, Sklar P, de Bakker PIW, Daly MJ, Sham PC. 2007. Plink: A tool set for whole-genome association and population-based linkage analyses. *The American Journal of Human Genetics* 81: 559–575.

Ralls K, Sunnucks P, Lacy RC, Frankham R. 2020. Genetic rescue: A critique of the evidence supports maximizing genetic diversity rather than minimizing the introduction of putatively harmful genetic variation. *Biological Conservation* 251: 108784.

Robins JH, McLenachan PA, Phillips MJ, Craig L, Ross HA, Matisoo-Smith E. 2008. Dating of divergences within the *Rattus* genus phylogeny using whole mitochondrial genomes. *Molecular Phylogenetics and Evolution* 49: 460–466.

Robins JH, Tintinger V, Aplin KP, Hingston M, Matisoo-Smith E, Penny D, Lavery SD. 2014. Phylogenetic species identification in *Rattus* highlights rapid radiation and morphological similarity of new Guinean species. *PLoS One* 9: e98002.

Rowe KC, Aplin KP, Baverstock PR, Moritz C. 2011. Recent and rapid speciation with limited morphological disparity in the genus *Rattus*. *Systematic Biology* 60: 188–203.

Schmieder R, Edwards R. 2011. Quality control and preprocessing of metagenomic datasets. *Bioinformatics* 27: 863–864.

Shirk AJ, Landguth EL, Cushman SA. 2017. A comparison of individual-based genetic distance metrics for landscape genetics. *Molecular Ecology Resources* 17: 1308–1317.

Simberloff D. 2013. *Invasive species: What everyone needs to know*. New York, USA: Oxford University Press.

Song Y, Endepols S, Klemann N, Richter D, Matuschka FR, Shih CH, Nachman MW, Kohn MH. 2011. Adaptive introgression of anticoagulant rodent poison resistance by hybridization between old world mice. *Current Biology* 21: 1296–1301.

Song Y, Lan ZJ, Kohn MH. 2014. Mitochondrial DNA phylogeography of the norway rat. *PLoS One* 9: e88425.

Tamura K, Stecher G, Kumar S. 2021. Mega11: Molecular evolutionary genetics analysis version 11. *Molecular Biology and Evolution* 38: 3022–3027.

Teng HJ, Zhang YH, Shi CM, Mao FB, Cai WS, Lu L, Zhao FQ, Sun ZS, Zhang JX. 2017. Population genomics reveals speciation and introgression between brown Norway rats and their sibling species. *Molecular Biology and Evolution* 34: 2214–2228.

Tigano A, Friesen VL. 2016. Genomics of local adaptation with gene flow. *Molecular Ecology* 25: 2144–2164.

Valencia-Montoya WA, Elfekih S, North HL, Meier JI, Warren IA, Tay WT, Gordon KHJ, Specht A, Paula-Moraes SV, Rane R, Walsh TK, Jiggins CD. 2020. Adaptive introgression across semipermeable species boundaries between local *Helicoverpa zea* and invasive *Helicoverpa armigera* moths. *Molecular Biology and Evolution* 37: 2568–2583.

Verneau O, Catzeflis F, Furano AV. 1998. Determining and dating recent rodent speciation events by using l1 (line-1) retrotransposons. *Proceedings of the National Academy of Sciences* 95: 11284–11289.

Weir BS, Cockerham CC. 1984. Estimating F-statistics for the analysis of population structure. *Evolution* 38: 1358–1370.

Wu XL, Mu DP, Yang QS, Zhang Y, Li YC, Feijó A, Cheng JL, Wen ZX, Lu L, Xia L, Zhou ZJ, Qu YH, Ge DY. 2023. Comparative genomics of widespread and narrow-range white-bellied rats in the *Niviventer niviventer* species complex sheds light on invasive rodent success. *Zoological Research* 44: 1052–1063.

Xie F, Wan T, Tang KY, Wang XM, Chen SD, Liu SY. 2022. Taxonomic and distribution revision of *Rattus pyctoris* in China. *Acta Theriologica Sinica* 42: 270–285.

Yu H, Jamieson A, Hulme-Beaman A, Conroy CJ, Knight B, Speller C, Al-Jarah H, Eager H, Trinks A, Adikari G, Baron H, Böhlendorf-Arslan B, Bohingamuwa W, Crowther A, Cucchi T, Esser K, Fleisher J, Gidney L, Gladilina E, Gol'din P, Goodman SM, Hamilton-Dyer S, Helm R, Hillman JC, Kallala N, Kivikero H, Kovács ZE, Kunst GK, Kyselý R, Linderholm A, Maraoui-Telmini B, Marković N, Morales-Muñiz A, Nabais M, O'Connor T, Oueslati T, Quintana Morales EM, Pasda K, Perera J, Perera N, Radbauer S, Ramon J, Rannamäe E, Sanmartí Grego J, Treasure E, Valenzuela-Lamas S, van der Jagt I, Van Neer W, Vigne JD, Walker T, Wynne-Jones S, Zeiler J, Dobney K, Boivin N, Searle JB, Krause-Kyora B, Krause J, Larson G, Orton D. 2022. Palaeogenomic analysis of black rat (*Rattus rattus*) reveals multiple European introductions associated with human economic history. *Nature Communications* 13: 2399.

## Supplementary Material

The following supplementary material is available online for this article at http://onlinelibrary.wiley.com/doi/10.1111/jse.13123/suppinfo:

**Fig. S1.** Representative skin specimens of the *Rattus* species examined in this study.

**Fig. S2.** Representative skull specimens of the *Rattus* species examined in this study.

**Fig. S3.** Morphological comparisons of the *Rattus* examined in this study.

**Fig. S4.** Neighbor-joining tree inferred using single nucleotide polymorphisms.

**Fig. S5.** TreeMix analysis results highlight the likelihood tree of *Rattus* species with the direction and degree of gene flow.

**Fig. S6.** OptM fit result map, which evaluated different m results of TreeMix.

**Table S1.** Origin measurements of the external morphology of the *Rattus* species examined in this study.

**Table S2.** Origin measurements of the craniodental morphology of the *Rattus* species examined in this study.

**Table S3.** Detailed information for localities of specimens for whole-genome sequencing.

**Table S4.** Collection information and accession number of data newly generated in this study for whole-genome sequencing.

**Table S5.** Accession numbers of additional SRA data in this study for whole-genome sequencing.

**Table S6.** Collection information and accession number of samples used for mitochondrial genome analysis.

**Table S7.** Accession numbers of samples from the National Center for Biotechnology Information (NCBI) used for mitochondrial genome analysis.

**Table S8.** Morphological data between species of *Rattus* in China: External and craniodental measurements.

**Table S9.** Gene flow between *Rattus* species tested by Dsuite.